# Underluminous 1991bg-like Type Ia supernovae are standardizable candles

O. Graur<sup>□</sup><sup>1,2</sup>\*

<sup>1</sup>Institute of Cosmology and Gravitation, University of Portsmouth, Portsmouth, PO1 3FX, UK

Accepted XXX. Received YYY; in original form ZZZ

#### **ABSTRACT**

It is widely accepted that the width-luminosity relation used to standardize normal Type Ia supernovae (SNe Ia) breaks down in underluminous, 1991bg-like SNe Ia. This breakdown may be due to the choice of parameter used as a stand-in for the width of the SN Ia light curve. Using the colour stretch parameter  $s_{\rm BV}$  instead of older parameters resolves this issue. Here, I assemble a sample of 14 nearby 1991bg-like SNe Ia from the literature, all of which have independent host-galaxy distance moduli and little to no reddening. I use Gaussian process regression to fit the light curves of these SNe in U/u, B, V, g, R/r, I/i, and H, and measure their peak absolute magnitudes. I find statistically significant (>  $5\sigma$  confidence level in the optical and >  $4\sigma$  in the near-infrared) correlations between the peak absolute magnitudes of the 1991bg-like SNe Ia and their  $s_{\rm BV}$  values in the range  $0.2 < s_{\rm BV} < 0.6$ . These correlations are broadly consistent with fits to  $s_{\rm BV} < 0.7$  SNe Ia with preliminary B- and V-band peak absolute magnitudes from the Carnegie Supernova Project and significantly inconsistent with similar fits to normal and transitional SNe Ia (with  $0.7 < s_{\rm BV} < 1.1$ ). The underluminous width-luminosity relation shown here needs to be properly calibrated with a homogeneous sample of 1991bg-like SNe Ia, after which it could be used as a rung on a new cosmological distance ladder. With surface-brightness fluctuations (or another non-Cepheid method) used to calibrate distances to nearby 1991bg-like SNe Ia, such a ladder could produce an independent measurement of the Hubble-Lemaître Constant,  $H_0$ .

**Key words:** methods: distance scale – supernovae: general

# 1 INTRODUCTION

Type Ia supernovae (SNe Ia) are famous for their use as standard candles, a use that led to the discovery of the accelerating expansion of the Universe and the existence of dark energy (Riess et al. 1998; Perlmutter et al. 1999). Yet, SNe Ia are not truly standard; they are *standardizable*. Independently, Rust (1974) and Pskovskii (1977) both showed that more luminous SNe Ia had wider light curves, i.e., they took longer to rise to peak and then decline. This correlation was corroborated and modernized by Phillips (1993) and has been in use ever since (for a historical review of the width-luminosity relation, see Phillips & Burns 2017; for a general review of the history and physics of SNe Ia, see Graur 2022).

Phillips (1993) found a tight correlation between the peak absolute luminosities of ten SNe Ia and the widths of their light curves, parameterized by  $\Delta m_{15}(B)$ , the number of magnitudes by which a SN Ia fades 15 days after it peaks in the *B* band. Variations on this parameter are now routinely used to fit SN Ia light curves and standardize them for use in cosmology. Examples include  $\Delta$ , used in MLCS2k2 (Jha et al. 2007); *s*, which is used in SALT and SiFT0 (Guy et al. 2005; Conley et al. 2008); and *x*1, used in SALT2 (Guy et al. 2007).

SNe are divided into several classes, each with its own subclasses. The same is true for SNe Ia. The majority of SNe Ia fall into the so-called 'normal' subclass, but there are also overluminous 1991T-like SNe Ia (Filippenko et al. 1992b), transitional 1986G-like SNe Ia

\* E-mail: or.graur@port.ac.uk

(Phillips et al. 1987), underluminous 1991bg-like SNe Ia (Filippenko et al. 1992a), peculiar SNe Iax (Jha et al. 2006b; Foley et al. 2013), and more. The width-luminosity relation works exceptionally well for normal SNe Ia and extends to overluminous 1991T-like and 1999aa-like SNe Ia as well (e.g., Burns et al. 2018; Yang et al. 2022). However, this relation breaks down in underluminous, fast-evolving 1991bg-like SNe (Burns et al. 2014). Consequently, these SNe Ia are routinely excised from cosmology samples, and the belief that '1991bg-like SNe Ia are not standard candles' has become dogma.

Burns et al. (2014) introduced a different stretch parameter,  $s_{\rm BV}$ , defined as the time at which the B-V colour curve reaches peak, relative to the time of B-band peak, divided by 30 days. When used as the basis for their own light-curve fitter, SNooPy (Burns et al. 2011), this parameter made it possible to standardize not just the light curves of normal and overluminous SNe Ia, but also underluminous SNe Ia as well (Burns et al. 2018). And yet, 1991bg-like SNe Ia are still not treated as standardizable candles. Some of this has to do with the continued use of light-curve fitters such as SALT2 and MLCS2k2, which are optimized for normal SNe Ia, and some of it has to do with the now deeply-ingrained belief that 1991bg-like SNe fall off the width-luminosity relation.

There are hints that the bias against 1991bg-like SNe may be starting to fade. Burns et al. (2018) and Hoogendam et al. (2022) noted that distances derived from the light curves of the 1991bg-like SNe 2006mr and 2015bo were consistent with independent distance measurements of their host galaxies (though see Stritzinger et al. 2010 and Dwomoh et al. 2023 for dissenting opinions on SN 2006mr).

<sup>&</sup>lt;sup>2</sup>Department of Astrophysics, American Museum of Natural History, Central Park West and 79th Street, New York, NY 10024-5192, USA

Table 1. SN sample: basic parameters

SN	Host	Class <sup>a</sup>	Redshift	$\Delta m_{15}(B)$ (mag)	$s_{\mathrm{BV}}$	$\mu^b$ (mag)	$E(B-V)_{ m MW}$ (mag)	$E(B-V)_{ m Host}$ (mag)
				Calib	ration sample			
1991bg	NGC 4374	Е	0.00339	1.88(0.10)	0.321(0.061)	31.23(0.02)	0.037	0.05(0.02)
1998de	NGC 0252	S0	0.01647	1.95(0.09)	0.351(0.120)	33.98(0.20)	0.052	0.00(0.00)
1999by	NGC 2841	Sab	0.00212	1.90(0.05)	0.381(0.063)	30.84(0.05)	0.010	0.020(0.030)
2005bl	NGC 4059	E	0.02392	2.00(0.06)	0.387(0.061)	35.21(0.11)	0.025	0.17(0.08)
2006mr	NGC 1316	Sab	0.00601	1.82(0.02)	0.239(0.060)	31.42(0.02)	0.018	0.089(0.039)
2007ax	NGC 2577	S0	0.00688	1.87(0.06)	0.355(0.061)	33.20(0.14)	0.045	< 0.01
2008R	NGC 1200	S0	0.01350	1.82(0.02)	0.591(0.060)	33.66(0.08)	0.062	0.009(0.013)
2015bo	NGC 5490	E	0.01614	1.91(0.01)	0.480(0.010)	34.27(0.08)	0.023	0.00(0.00)
2017ejb	NGC 4696	E	0.00990	2.04(0.04)	0.470(0.010)	32.88(0.06)	0.097	0.05(0.02)
2019so	NGC 4622	Sa	0.01457	1.96(0.04)	0.410(0.010)	34.27(0.48)	0.128	-0.01(0.02)
2021qvv	NGC 4442	S0	0.00183	2.05(0.03)	0.280(0.050)	30.85(0.07)	0.019	0.00(0.00)
				Te	est sample			
1997cn	NGC 5490	Е	0.01614	1.90(0.05)	0.350(0.060)	34.27(0.08)	0.023	0.00(0.00)
1999da	NGC 6411	E	0.01269	1.94(0.10)	0.442(0.160)	33.12(0.27)	0.046	0.00(0.00)
2022xkq	NGC 1784	SBc	0.00773	1.65(0.03)	0.630(0.030)	32.14(0.12)	0.119	0.00(0.00)

<sup>&</sup>lt;sup>a</sup>Galaxy classifications sourced from de Vaucouleurs et al. (1991).

Burns et al. (2018) showed that a quadratic function provided a good fit to absolute magnitudes of both normal and fast-declining SNe Ia across the optical and near-infrared, and that derivations of the Hubble-Lemaître constant,  $H_0$ , remained consistent whether SNe Ia with  $s_{\rm BV} > 0.5$  were excluded or not. And yet, many cosmological analyses continue to exclude underluminous and fast-declining SNe Ia (e.g., Vincenzi et al. 2024; DES Collaboration et al. 2024).

In this paper, I set out to independently test whether there is a correlation between the luminosities of 1991bg-like SNe Ia and the widths of their light curves, as parameterized by  $s_{BV}$ . In Section 2, I assemble a sample of 14 1991bg-like SNe Ia that suffered little to no dust extinction and that exploded in galaxies with independent distance measurements. Since all SN Ia light-curve fitters are optimized towards normal SNe Ia, in Section 3 I fit the light curves of the SNe myself with Gaussian process regression (GPR). The results, shown in Section 4, are clear: there are statistically significant correlations between the peak absolute magnitudes of 1991bg-like SNe Ia and  $s_{\rm BV}$  in multiple filters (B, V, g, R/r, I/i, and H). This leads to Section 5, in which I discuss the potential use of 1991bg-like SNe Ia in a new distance ladder, independent from the one currently dominating SN Ia cosmology.

#### 2 SAMPLE

A review of the literature on 1991bg-like SNe Ia revealed that only ~ 30 such objects had been methodically observed and published. Of these, only 14 had a spectroscopic classification, well-sampled multiwavelength light curves, exploded in galaxies with independent distance measurements, and suffered relatively little host-galaxy dust extinction (E(B-V) < 0.2 mag). The latter is important because most estimates of host-galaxy extinction are a byproduct of lightcurve fitting, which I avoid in this paper. The SN sample used in this work is shown in Table 1.

Of the 14 SNe, 11 are used to test for the presence of a widthluminosity relation, while the other three SNe are held back as test cases (Section 4.3). All of the SNe in this sample were spectroscopically classified as 1991bg-like SNe Ia by various authors, either based on the appearance of the telltale Ti II band at 400-440 nm or by comparing their spectra to different SN Ia spectroscopic templates (e.g., using SNID; Blondin & Tonry 2007). Below, I describe the sources of the light curves used in this work. Basic parameters of the SNe in the sample, including the names and types of galaxies in which they exploded, are summarized in Table 1.

The eponymous SN 1991bg was extensively studied by Filippenko et al. (1992a), Leibundgut et al. (1993), and Turatto et al. (1996). Here, I use the peak magnitudes reported by Turatto et al. (1996), based on a combined analysis of their data and those of Filippenko et al. (1992a) and Leibundgut et al. (1993). UBVRI observations of SN 1997cn were published by Turatto et al. (1998) and Jha et al. (2006a). Modjaz et al. (2001) and Jha et al. (2006a) published BVRI light curves of SN 1998de, obtained as part of the Lick Observatory Supernova Search (LOSS; Filippenko et al. 2001). UBVRIJHK observations of SN 1999by were published by Garnavich et al. (2004), who presented an in-depth study of this object. Additional BVRI observations, obtained by LOSS, were published by Ganeshalingam et al. (2010), while three additional epochs of JHK observations were obtained by Höflich et al. (2002). BVI and BVRI observations of SN 1999da were published by Krisciunas et al. (2001) and Ganeshalingam et al. (2010), respectively. Here, I use the latter as they contain the additional R filter.

The Carnegie Supernova Project (CSP; Contreras et al. 2010; Stritzinger et al. 2011; Krisciunas et al. 2017) have published uBVgriYJH observations of 16 underluminous, 1991bg-like SNe Ia. Of these, only the host galaxies of SNe 2005bl, 2006mr, 2007ax, and 2008R had independent distance measurements and host-galaxy reddening < 0.2 mag (Burns et al. 2014). An independent analysis of SN 2005bl (Taubenberger et al. 2008) estimated a host-galaxy reddening of  $0.17 \pm 0.08$  mag and an  $R_V$  value of 3.1, which I use here. Additional observations of SN 2007ax were published by Kasliwal et al. (2008), who also estimated a negligible host-galaxy reddening of < 0.01 mag.

<sup>&</sup>lt;sup>b</sup> All distance moduli are weighted averages of measurements from the literature and independent of distance measurements derived from SN Ia light-curve fitting.

SN 2017ejb was studied by Hoogendam et al. (2022) in *uBV griH*. SN 2017ejb was spectroscopically classified as a 1991bg-like SN Ia by Pan et al. (2017) and Valenti et al. (2017). SN 2019so was classified as a 1991bg-like SN Ia by Olivares et al. (2019). *BVri* observations of both SNe were obtained with the Las Cumbres Observatory's network of 1-m telescopes (Brown et al. 2013) and reported by Chen et al. (2022).

Spectra and *UBV griJH* images of SN 2021qvv were obtained as part of the Las Cumbres Observatory's Global Supernova Project and published by Graur et al. (2023). The latter classified it as a 1991bg-like SN Ia similar to SN 2006mr. *UBV griJHK* observations of SN 2022xkq were published by Pearson et al. (2024), who performed an in-depth analysis of this object.

#### 3 ANALYSIS

Here, I describe the steps taken to measure the peak absolute magnitudes of the SNe in my sample: measuring  $s_{\rm BV}$  (Section 3.1), obtaining the distance moduli of the SN host galaxies (Section 3.2) and the reddening suffered by the SNe (Section 3.3), and measuring peak apparent and absolute magnitudes (Section 3.4).

#### 3.1 Colour stretch

SNe 1997cn, 2005bl, 2006mr, 2007ax, 2008R, 2015bo, 2017ejb, 2019so, and 2022xkq have been fit with SNooPy by other authors (Burns et al. 2014; Krisciunas et al. 2017; Hoogendam et al. 2022; Chen et al. 2022). For these SNe, I use the published  $s_{BV}$  values. For the rest of the sample (namely, SNe 1991bg, 1998de, 1999by, 1999da, and 2021qvv), I have derived  $s_{BV}$  by fitting their light curves with GPR fits, as done by Graur et al. (2023). To ensure that the GPRderived s<sub>BV</sub> values are not systematically offset from the SNooPyderived values, I use GPR to fit the light curves of 16 1991bg-like SNe Ia observed by CSP (SNe 2005bl, 2005ke, 2006gt, 2006mr, 2007N, 2007ax, 2007ba, 2008R, 2009F, 2006bd, 2006hb, 2007al, 2007jh, 2008bd, 2008bi, and 2008bt) and compare my values to those published by Krisciunas et al. (2017). As Fig. 1 shows, there is a tight correlation between the two techniques, with  $s_{BV}(SNooPy) =$  $(0.95 \pm 0.14)s_{BV}(GPR) - (0.06 \pm 0.08)$  and a reduced  $\chi_r^2$  value of 15.2/14 = 1.1. The GPR-derived  $s_{BV}$  values of the pre-2000 SNe have been corrected accordingly. The resultant  $s_{BV}$  values, along with  $\Delta m_{15}(B)$  measurements from the literature, are presented in Table 1.

## 3.2 Distance moduli

No single work on nearby distance moduli encompasses all of the host galaxies in my sample. Instead of picking and choosing between the various measurements available for each galaxy, I take a weighted mean of all measurements conducted from the year 2000 onwards. For some host galaxies, which have > 10 measurements, this results in an underestimated uncertainty on the distance modulus. I do not include distance modulus measurements derived from fitting the light curves of the SNe in the sample, for two reasons. First, this would be cyclical reasoning, as the goal of this paper is to ascertain whether 1991bg-like SNe Ia can be used as standardizable candles. Second, as Graur et al. (2023) noted, because current light-curve fitters are not optimized for 1991bg-like SNe Ia, the distance moduli derived in this manner often span a range of ~ 1 mag (see Section 4.3, below). The sources of the measurements used for each host galaxy

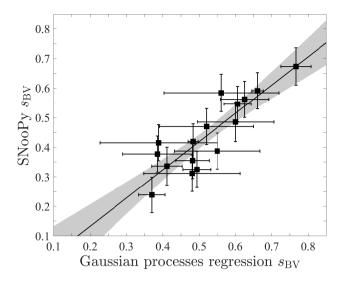


**Figure 1.**  $s_{\rm BV}$  values derived with GPR are  $\approx 5$  per cent larger than the values derived by the SNooPy light-curve fitter. The correlation shown here is  $s_{\rm BV}({\rm SNooPy}) = (0.95 \pm 0.14) s_{\rm BV}({\rm GPR}) - (0.06 \pm 0.08)$  with a reduced  $\chi_{\pi}^2$  value of 1.1.

are gathered in Appendix A, and the resultant distance moduli and their uncertainties are collected in Table 1.

## 3.3 Reddening

Galactic line-of-sight reddening towards the SNe in the sample,  $E(B-V)_{MW}$ , were extracted from the reddening maps produced by Schlafly & Finkbeiner (2011), while host-galaxy reddening values,  $E(B-V)_{Host}$ , were extracted from the literature (see Section 2). Unlike Galactic reddening, host-galaxy reddening is derived from light-curve fits. Since most light-curve fitters are not optimized towards fitting 1991bg-like light curves, these values are suspect. Thus, I chose to include only SNe whose literature  $E(B - V)_{Host}$ values were < 0.1 mag. The sole exception is SN 2005bl, with  $E(B-V)_{\text{Host}} = 0.17 \pm 0.08 \text{ mag}$  (Taubenberger et al. 2008). As it exploded in an elliptical galaxy, I chose to keep it in the sample. To avoid any systematic uncertainties that have to do with how hostgalaxy reddening and  $R_V$  values are derived, and since, by design, the host-galaxy reddenings are low, I chose not take them into account in the following analysis. A test in which these values were included in the derivation of the peak absolute magnitudes showed that including them did not impact the results in a significant manner.

#### 3.4 Peak magnitudes

Here, I follow Graur et al. (2023) and fit the light curves of the SNe in my sample using the Matlab 2023a GPR-fitting routine fitrgp with the default parameters. These fits provide the date and magnitude of maximum light in each of seven filters: U/u, B, V, g, R/r, I/i, and H. While some of the SNe in my sample had YJHK observations, most of these observations were obtained after the SNe had already peaked in these bands; the H band was the only one of these filters in which there were more than two SNe with pre- and post-peak observations required for the GPR-fitting routine to estimate peak magnitudes.

To estimate the uncertainties on the derived parameters, I repeat the fit in each filter 100 times, each time varying the photometry of the SN randomly according to the measurement uncertainties. The mean and standard deviation of the results are then taken as the estimated peak date and its  $1\sigma$  uncertainty. The same method is applied to estimating the peak apparent magnitude in each filter. Magnitude uncertainties smaller than 0.01 mag are rounded up. The resultant peak apparent magnitudes are presented in Table 2.

In Fig. 2, I compare the peak apparent magnitudes derived using this method with published values from the literature, derived using various fitting techniques. In all filters, except U/u, the mean difference between the GPR and literature values is  $\leq 0.06$  mag. In U/u, this value rises to 0.1 mag, but this is due to a single outlier, SN 2005bl.

With the fitted peak apparent magnitudes, Galactic reddening values, and distance moduli described above, the peak absolute magnitude of the i-th SN in my sample in filter  $\lambda$  is simply:

$$M(\lambda)_{\max,i} = m(\lambda)_{\max,i} - A(\lambda)_i - \mu_i, \tag{1}$$

where  $\mu_i$  is the distance modulus of the i-th SN, and  $A(\lambda)_i$  is derived from the Galactic line-of-sight reddening,  $E(B-V)_{\mathrm{MW},i}$ , the Galaxy's  $R_V=3.1$ , and the Cardelli et al. (1989) extinction law. Due to the nature of the SN sample, which includes SNe observed by different surveys in different filters (e.g., U/u, R/r, and I/i), I do not attempt to perform K or S corrections. The resultant peak absolute magnitudes are presented in Table 3 and Fig. 3.

#### 4 RESULTS

Here, I fit the peak absolute magnitudes measured in the previous section and show that correlations between them and the colour stretch of the SNe are statistically significant in all filters except U/u (Section 4.1); compare these correlations to fits applied to independent CSP data (Section 4.2); and demonstrate the effect of these correlations on our understanding of SNe 1997cn, 1999da, and 2022xkq (Section 4.3).

## 4.1 Width-luminosity relations

I perform two independent tests to determine whether the peak absolute magnitudes in a specific filter are correlated with colour stretch,  $s_{\rm BV}$ , the results of which are collected in Table 4. First, all filters display a strong, negative Pearson correlation coefficient, r, with  $r \leq -0.9$  in B, V, g, R/r, and H, and  $r \sim -0.7$  in U/u and I/i. The same test shows that these correlations have statistically significant p-values of < 0.05 in all filters except U/u (and a more stringent p < 0.01 in all filters except U/u and I/i). Second, a likelihood-ratio test (see, e.g., Graur et al. 2017a) prefers a 1st-order polynomial over a 0th-order polynomial fit to the data in every filter with a statistical significance of  $> 5\sigma$ . The same test shows that a 2nd-order polynomial is not preferred over a 1st-order polynomial.

Based on the likelihood-ratio test, I fit 1st-order polynomials to the peak absolute magnitudes in each filter, the results of which are presented in Table 4 and Fig. 3. An analysis of the residuals produced by subtracting the best-fitting polynomials from the data reveals a scatter, S, of < 0.3 mag in all filters except U/u, and < 0.2 mag in B, V, and H. I attribute the high scatter in U/u to the difficulty in estimating the time of peak from photometry that, only in this band, did not always cover the rise and peak of the light curves (SNe 1999by, 2007ax, 2008R, and 2021qvv). Note that, even without K and S corrections, and with distance moduli derived using a variety of techniques, the scatter found here is on par with, or better than, the scatter found in the initial width-luminosity relations measured by Phillips (1993) for normal SNe Ia.

It is instructive to note that the width-luminosity relation in the H

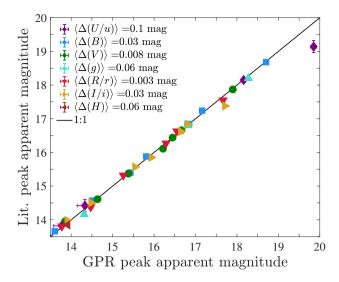


Figure 2. Peak apparent magnitudes derived with GPR are in good agreement with similar values derived by previous works with various light-curve fitters. The solid curve represents the 1:1 line, and the various symbols and colors represent the seven filters tested here (see legend). In six of the seven filters, the mean difference between the GPR and literature values is  $\leq 0.06$  mag. Only in U/u, where the light curves are sparsest, does the mean difference between the values rise to 0.1 mag, due to a single outlier, SN 2005bl.

band is similar in nature to the optical correlations. This is not the case in normal SNe Ia, which exhibit a smaller scatter in luminosity in the NIR than in the optical (e.g., Avelino et al. 2019). However, a larger NIR sample is required to validate this statement, as the quadratic fits shown in figure 4 of Burns et al. (2018) hint at a reduction in the NIR luminosity scatter similar to that seen in normal SNe Ia.

# 4.2 Comparison with CSP

In Fig. 4, I compare my *B*- and *V*-band measurements to similar CSP peak absolute magnitudes from Hoogendam et al. (2022). These measurements are preliminary (the finalized CSP measurements will appear in the published version of Uddin et al. 2023; W. B. Hoogendam, private communication) but provide a good sanity test and the option to compare the correlations found above with the well-established width-luminosity relation of normal SNe Ia.

The *B*-band CSP data were obtained by fitting the light curves with SNooPy using the EBV2 model, while the *V*-band peak absolute magnitudes were obtained via GPR fits, which explains the larger scatter in this filter (Hoogendam et al. 2022). To recreate figure 9 from Hoogendam et al. (2022), I have removed all *V*-band measurements with uncertainties  $\sigma[M(V)] > 0.3$  mag and  $\sigma(s_{\rm BV}) > 0.06$  (Hoogendam et al. 2022 used a stricter  $\sigma(s_{\rm BV}) > 0.05$ , but my sample has an average  $\langle \sigma(s_{\rm BV}) \rangle \sim 0.06$ ). No cuts were applied to the *B*-band data

A likelihood-ratio test applied to the entire range of CSP data in the B band prefers a 2nd-order polynomial over a 1st-order polynomial at a >  $5\sigma$  confidence level, indicating that the underluminous SNe Ia follow a different trend than the normal ones. This is consistent with Burns et al. (2018). However, a visual inspection of the 2nd-order polynomial fit, shown in Fig. 4, reveals that it underestimates the absolute magnitudes in the range  $0.55 \lesssim s_{\rm BV} \lesssim 0.75$ . In other words, it does not manage to recreate the sharp break between normal and underluminous SNe Ia. The same likelihood-ratio test conducted on the V-band CSP measurements finds no statistically significant

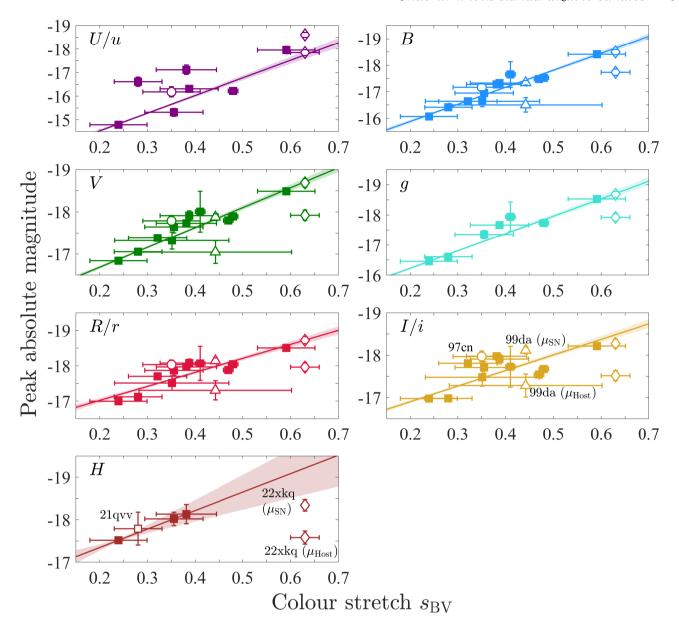


Figure 3. Peak absolute magnitude vs. colour stretch,  $s_{\rm BV}$ . Magnitudes have been corrected for Galactic line-of-sight reddening. The shaded regions around the linear fits represent the  $1\sigma$  uncertainties of the fits. The correlations, calculated using the calibration sample (filled squares) are statistically significant in all filters except U/u. SNe 1997cn, 1999da, and 2022xkq (described in detail in Section 4.3) are shown as an open circle, triangle, and diamond, respectively. SNe 1999da and 2022xkq are shown twice, once when using a host-based distance modulus ( $\mu_{\rm Host}$ ) and once when using a distance modulus derived by SN light-curve fitters ( $\mu_{\rm SN}$ ). For clarity, the second measurements of SNe 1999da and 2022xkq are shown without their horizontal error bars. The H-band measurement of SN 2021qvv, shown as an open square, is not used in the fit.

preference for a 2nd-order polynomial over a 1st-order polynomial, or even for a 1st-order polynomial over a 0th-order polynomial.

Based on the results of the likelihood-ratio test on the *B*-band CSP data, I fit the CSP measurements in both filters with 1st-order polynomials in two  $s_{\rm BV}$  ranges:  $0.7 < s_{\rm BV} < 1.1$  to capture all normal SNe Ia (as well as transitional SNe Ia), and  $s_{\rm BV} < 0.7$  to include only underluminous SNe Ia. In the *B* band, I find that the normal SNe Ia follow  $M(B)_{\rm CSP} = (-1.5 \pm 0.1) s_{\rm BV} - (17.9 \pm 0.1) (\chi^2 = 5.7/42 = 0.14)$  and underluminous SNe Ia follow  $M(B)_{\rm CSP} = (-5.3 \pm 0.2) s_{\rm BV} - (15.5 \pm 0.1) (\chi^2 = 22/9 = 2.4)$ . In the *V* band, the correlations are  $M(V)_{\rm CSP} = (-1.8 \pm 0.1) s_{\rm BV} - (17.2 \pm 0.1) (\chi^2 = 1010/55 = 18)$  and  $M(V)_{\rm CSP} = (-4.0 \pm 0.2) s_{\rm BV} - (15.7 \pm 0.1) (\chi^2 = 498/15 = 33)$ ,

respectively. The higher  $\chi^2$  values, divided by the number of degrees of freedom, are due to the larger scatter of the measurements in this filter.

Overplotting the *B*- and *V*-band peak absolute magnitudes from Fig. 3 shows that the width-luminosity relations from my sample are in broadly good agreement with the fits to the CSP data. This is somewhat surprising, given the heterogeneity of my sample, the variety of methods used to derive distance moduli to the SN host galaxies, and the lack of *K* corrections. It is too much to assume that all of these factors would conspire to produce correlations that coincidentally agreed with the homogeneous, well-calibrated CSP data. Instead, we must conclude that there are, indeed, clear correlations

Table 2. Peak apparent magnitudes

SN	$m(U/u)_{\max}$ (mag)	$m(B)_{\max}$ (mag)	$m(V)_{\max}$ (mag)	$m(g)_{\max}$ (mag)	$m(R/r)_{\rm max}$ (mag)	$m(I/i)_{ m max}$ (mag)	$m(H)_{\max}$ (mag)
			Calibration	n sample			
1991bg		14.75(0.10)	13.96(0.05)		13.63(0.05)	13.50(0.05)	
1998de		17.56(0.04)	16.82(0.04)		16.61(0.04)	16.61(0.05)	
1999by	13.77(0.19)	13.60(0.01)	13.14(0.01)		12.90(0.01)	12.89(0.01)	12.71(0.22)
2005bl	19.85(0.07)	18.70(0.02)	17.90(0.02)	18.28(0.02)	17.66(0.03)	17.71(0.03)	
2006mr	16.72(0.03)	15.43(0.04)	14.64(0.01)	15.03(0.01)	14.47(0.05)	14.48(0.01)	13.91(0.01)
2007ax	18.10(0.09)	16.44(0.02)	15.69(0.02)	16.02(0.03)	15.45(0.01)	15.59(0.01)	15.21(0.07)
2008R	16.01(0.13)	15.51(0.01)	15.37(0.01)	15.37(0.01)	15.32(0.01)	15.58(0.02)	
2015bo	18.16(0.04)	16.85(0.01)	16.45(0.01)	16.62(0.01)	16.29(0.01)	16.65(0.02)	
2017ejb		15.81(0.02)	15.38(0.02)		15.26(0.02)	15.54(0.02)	
2019so		17.16(0.03)	16.66(0.02)	16.81(0.08)	16.55(0.02)	16.81(0.04)	
2021qvv	14.33(0.19)	14.51(0.01)	13.85(0.01)	14.31(0.03)	13.78(0.01)	13.91(0.02)	$13.07(0.38)^a$
			Test sar	mple			
1997cn (GPR)	18.20(0.20)	17.20(0.10)	16.55(0.10)		16.30(0.10)	16.35(0.10)	
1997cn (2007ax)	18.23(0.20)	17.16(0.10)	16.41(0.10)	16.74(0.03)	16.17(0.10)	16.31(0.10)	
1999da		16.81(0.03)	16.22(0.01)		15.94(0.02)	15.93(0.02)	
2022xkq	14.87(0.02)	14.91(0.01)	14.58(0.01)	14.67(0.01)	14.50(0.01)	14.87(0.01)	14.63(0.09)

<sup>&</sup>lt;sup>a</sup>The H-band peak magnitude of SN 2021qvv was derived by Graur et al. (2023) using the SNooPy light-curve fitter and a single *H*-band measurement of  $13.16 \pm 0.06$  mag obtained 0.6 d past *B*-band maximum light (see Section 4.3.3).

Table 3. Peak absolute magnitudes

SN	$M(U/u)_{\max}$ (mag)	$M(B)_{\max}$ (mag)	$M(V)_{\max}$ (mag)	$M(g)_{\max}$ (mag)	$M(R/r)_{\text{max}}$ (mag)	$M(I/i)_{ m max}$ (mag)	$M(H)_{ m max}$ (mag)
			Calibration	sample			
1991bg		-16.64(0.10)	-17.38(0.05)		-17.70(0.05)	-17.81(0.05)	
1998de		-16.64(0.20)	-17.32(0.20)		-17.51(0.20)	-17.48(0.21)	
1999by	-17.12(0.20)	-17.28(0.05)	-17.73(0.05)		-17.97(0.05)	-17.97(0.05)	-18.13(0.23)
2005bl	-16.31(0.13)	-17.33(0.11)	-17.91(0.11)	-17.67(0.11)	-18.07(0.11)	-17.91(0.11)	
2006mr	-14.79(0.04)	-16.07(0.04)	-16.84(0.02)	-16.46(0.02)	-17.00(0.06)	-16.98(0.02)	-17.52(0.02)
2007ax	-15.32(0.17)	-16.95(0.14)	-17.65(0.14)	-17.35(0.14)	-17.87(0.14)	-17.71(0.14)	-18.02(0.16)
2008R	-17.95(0.13)	-18.41(0.08)	-18.49(0.08)	-18.53(0.08)	-18.51(0.08)	-18.21(0.08)	
2015bo	-17.52(0.08)	-16.22(0.09)	-17.74(0.08)	-17.89(0.08)	-18.04(0.08)	-17.67(0.08)	
2017ejb		-17.48(0.06)	-17.80(0.06)		-17.88(0.06)	-17.54(0.06)	
2019so		-17.65(0.48)	-18.01(0.48)	-17.94(0.49)	-18.07(0.48)	-17.73(0.48)	
2021qvv	-16.61(0.20)	-16.42(0.07)	-17.05(0.07)	-16.61(0.07)	-17.12(0.07)	-16.98(0.07)	$-17.79(0.39)^a$
			Test sar	nple			
1997cn (GPR)	-16.18(0.22)	-17.17(0.13)	-17.79(0.13)	• • • • •	-18.03(0.13)	-17.97(0.13)	
1997cn (2007ax)	-16.16(0.22)	-17.21(0.13)	-17.93(0.13)	-17.62(0.09)	-18.16(0.13)	-18.01(0.13)	
1999da ( $\mu_{\mathrm{Host}}$ )		-16.51(0.27)	-17.05(0.27)		-17.31(0.27)	-17.28(0.27)	
1999da ( $\mu_{\rm SN}$ )		-17.34(0.08)	-17.88(0.08)		-18.14(0.08)	-18.12(0.08)	
2022xkq ( $\mu_{\text{Host}}$ )	-17.84(0.12)	-17.73(0.12)	-17.92(0.12)	-17.92(0.12)	-17.96(0.12)	-17.52(0.12)	-17.58(0.15)
2022xkq ( $\mu_{\rm SN}$ )	-18.60(0.10)	-18.49(0.10)	-18.68(0.10)	-18.68(0.10)	-18.72(0.10)	-18.28(0.10)	-18.34(0.14)

<sup>&</sup>lt;sup>a</sup>The H-band peak magnitude of SN 2021qvv was derived by Graur et al. (2023) using the SNooPy light-curve fitter and a single *H*-band measurement of  $13.16 \pm 0.06$  mag obtained 0.6 d past *B*-band maximum light (see Section 4.3.3).

between the peak absolute magnitudes of 1991bg-like SNe Ia and the widths of their light curves, as parameterized by  $s_{BV}$ .

### 4.3 Test cases

When constructing the SN sample in Section 2, the underluminous SNe 1997cn and 1999da were set aside. Below, I describe the circumstances that led me to isolate each of these SNe and how they help validate the width-luminosity relations from Section 4.1. I also

discuss the H-band peak absolute magnitude of SN 2021qvv as well as the absolute magnitudes of SN 2022xkq, whose situation is similar to that of SN 1999da.

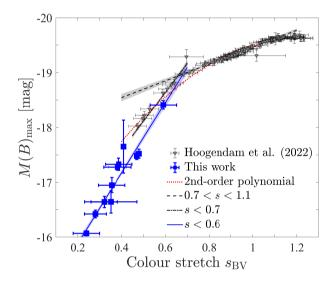
### 4.3.1 SN 1997cn

SN 1997cn was observed by both Turatto et al. (1998) and Jha et al. (2006a), but only after it had already peaked and begun to decline. Turatto et al. (1998) estimated that the SN reached B-band maximum

**Table 4.**  $M-s_{\rm BV}$  correlation parameters

Filter	a (mag)	b (mag)	$\chi_r^2$	$L \over (\sigma)$	r	p	S (mag)
U/u	-7.5(0.2)	-13.0(0.1)	26	5	-0.72	$6.6 \times 10^{-2}$	0.74
$\boldsymbol{B}$	-6.4(0.2)	-14.6(0.1)	3.9	5	-0.96	$4.1 \times 10^{-6}$	0.19
V	-4.7(0.2)	-15.8(0.1)	3.9	5	-0.93	$4.4 \times 10^{-5}$	0.18
g	-5.8(0.2)	-15.1(0.1)	1.6	5	-0.95	$1.1 \times 10^{-3}$	0.23
R/r	-4.0(0.2)	-16.2(0.1)	7.9	5	-0.88	$3.1 \times 10^{-4}$	0.21
I/i	-3.7(0.2)	-16.2(0.1)	23	5	-0.72	$1.2 \times 10^{-2}$	0.28
H	-4.3(1.0)	-16.5(0.3)	$7 \times 10^{-4}$	4	-1.0	$2.6 \times 10^{-3}$	$1.4 \times 10^{-3}$

Columns are: (1) filter; (2 + 3) best-fitting parameters for a first-order polynomial  $M = as_{\rm BV} + b$  (uncertainties appear in parentheses); (4) reduced  $\chi^2$  of fit; (5) significance of likelihood-ratio test; (6 + 7) Pearson r coefficient and its p-value; and (8) scatter after subtracting the best-fitting polynomial from the data.



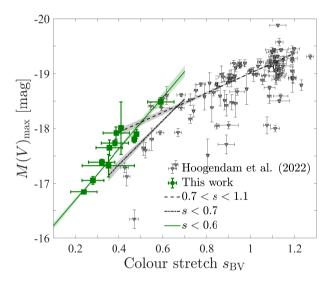


**Figure 4.** Absolute *B*- (left) and *V*-band (right) magnitudes vs. colour stretch,  $s_{\rm BV}$  for the 1991bg-like SNe Ia used to calibrate the width-luminosity relations in this work (blue and green squares, respectively) and CSP SNe Ia (gray triangles; preliminary measurements shown in Hoogendam et al. 2022, with finalised measurements expected in Uddin et al. 2023). The dashed, black curves represent 1st-order polynomial fits to normal and transitional SNe Ia ( $0.7 < s_{\rm BV} < 1.1$ ), while the dot-dashed, black curves were fit to CSP SNe Ia with  $s_{\rm BV} < 0.7$ . The red, dotted curve is a 2nd-order polynomial fit to all of the CSP data. As detailed in the text, the normal and underluminous SN Ia curves have significantly different slopes. On the other hand, the slopes of the fits to the peak absolute magnitudes measured here (blue and green solid curves, respectively) are broadly consistent with those of the underluminous CSP SNe Ia.

light on JD 2450587.5, while Hoogendam et al. (2022) used SNooPy to fit the Jha et al. (2006a) light curves and derive a peak date of  $2450580.7 \pm 0.7$ , 6.8 d earlier than the Turatto et al. (1998) date and  $\sim 2$  d prior to its discovery (Li et al. 1997). A spectroscopic fit with SNID yielded a third date: 2450588.3, 0.8 d after the Turatto et al. (1998) estimate. As the light curves of this SN did not cover the date of maximum light, I did not include it in my sample.

The SNooPy fit conducted by Hoogendam et al. (2022) provided an  $s_{\rm BV}$  value of 0.35  $\pm$  0.06. As this value is consistent with the  $s_{\rm BV}$  value of SN 2007ax, 0.355  $\pm$  0.061 (Krisciunas et al. 2017), the light curves of the two SNe can be compared to each other directly. In Fig. 5, I fit the *V*-band measurements of SN 2007ax to those of SN 1997cn taken by both Turatto et al. (1998) and Jha et al. (2006a) by varying the date of maximum light and the offset between the light curves. I find  $t(B)_{\rm max} = 2450586.1 \pm 0.2$  d, with SN 1997cn 0.72  $\pm$  0.01 mag fainter than SN 2007ax, with a reduced  $\chi_r^2 = 2.1$ .

Fig. 3 includes peak absolute magnitudes of SN 1997cn estimated by adding an offset of 0.72 mag to the peak apparent magnitudes of SN 2007ax. The resultant values are consistent with peak apparent

magnitudes estimated by GPR fits to the data from Jha et al. (2006a), with the exception of the g band, in which there were no previous measurements. In all filters, the resultant peak absolute magnitudes of SN 1997cn are consistent with the width-luminosity relations within the scatter of the calibration sample. This indicates that the width-luminosity relations measured in Section 4.1 can be used to estimate the peak absolute magnitudes of individual 1991bg-like SNe Ia.

## 4.3.2 SN 1999da

The host galaxy of SN 1999da only had two independent, post-2000 distance measurements (both from Blakeslee et al. 2001), which averaged to  $\mu_{\rm Host} = 33.12 \pm 0.27$  mag. However, distance moduli derived by fitting the light curves of this SN by various groups (Riess et al. 2004; Wang et al. 2006; Jha et al. 2007; Kowalski et al. 2008; Hicken et al. 2009), using different light-curve fitters, produced an average value of  $\mu_{\rm SN} = 33.95 \pm 0.08$ ,  $\sim 0.8$  mag fainter. Fig. 3 shows SN 1999da twice, using each of the distance moduli above. In all four filters in which this SN was observed, the peak

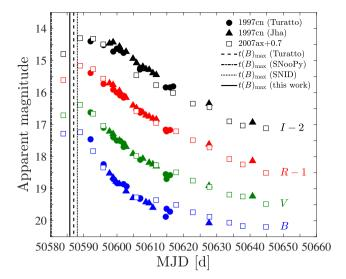


Figure 5. A comparison between SN 1997cn (filled circles and triangles from Turatto et al. 1998 and Jha et al. 2006a, respectively) and SN 2007ax (empty squares; Krisciunas et al. 2017). Derived dates of maximum light are shown as dashed (Turatto et al. 1998), dot-dashed (SNooPy; Hoogendam et al. 2022), dotted (SNID; Hoogendam et al. 2022), and solid (this work) curves. According to the fit between the two SNe, SN 1997cn was  $\approx 0.7$  mag dimmer than SN 2007ax.

absolute magnitudes derived using the host-based distance modulus are systematically dimmer than the width-luminosity relations. The peak absolute magnitudes derived with the light-curve-based distance modulus, on the other hand, are consistent with the correlations. This indicates that, at least for this SN, existing light-curve fitters already did a good job of deriving its luminosity distance.

# 4.3.3 SN 2021qvv

Only one epoch of JH observations was obtained for SN 2021qvv, 0.6 d after B-band maximum light. A SNooPy fit determined that the SN peaked in the H band  $\sim 4$  d later, and that the peak magnitude was  $13.07 \pm 0.38$  mag,  $\sim 0.9$  mag brighter than the sole H-band measurement (Graur et al. 2023). I did not use this light-curve-fitter derived magnitude to fit the correlation between the H-band absolute magnitudes and  $s_{\rm BV}$ , yet, when plotted in Fig. 3, it is fully consistent with the H-band correlation.

## 4.3.4 SN 2022xkq

The host galaxy of SN 2022xkq has several distance modulus measurements (Table A1), which provide a weighted average of  $\mu_{\rm Host} = 32.14 \pm 0.12$  mag. However, as in the case of SN 1999da, a SNooPy fit provides a  $\sim 0.8$  mag fainter distance modulus of  $\mu_{\rm SN} = 32.9 \pm 0.1$  mag (Pearson et al. 2024). Once again, I use both distance moduli to plot the absolute magnitudes of this SN in Fig. 3. Exactly as before, the absolute magnitudes derived using the light-curve-based distance modulus are consistent with the correlations (in the U/u band, both distance moduli result in absolute magnitudes that are consistent with the scatter around the correlation, while in the H band, the light-curve-based absolute magnitude is consistent with the correlation within  $2\sigma$ ). This provides another indication that light-curve fitters, and especially SNooPy, are already capable of standardizing 1991bg-like SNe Ia.

#### **5 CONCLUSIONS**

In this work, I have assembled a sample of 14 underluminous, 1991bg-like SNe Ia from the literature to test whether this type of SN Ia can be used as a standardizable candle, as previously noted by Burns et al. (2018) for fast-declining SNe Ia in general. To minimize systematic uncertainties, I have chosen SNe Ia that exploded in host galaxies with independent distance moduli, low to no reddening, and well-sampled light curves. Even so, the sample still suffers from systematic uncertainties that stem from the variety of filters in which the SNe were observed as well as a lack of K and S corrections. This sample still exhibits statistically significant ( $>5\sigma$ ) correlations between the peak absolute magnitudes of the 1991bg-like SNe Ia and the widths of their light curves, as parameterized by the colour stretch,  $s_{\rm BV}$ .

The 1991bg-like SN Ia width-luminosity relations measured here are similar in nature to those of normal SNe Ia but with significantly steeper slopes. The *B*- and *V*-band width-luminosity relations are consistent with preliminary CSP data, which both strengthens the existence of the correlations and shows that SNooPy, the light-curve fitter used by CSP, is able to standardize underluminous as well as normal SNe Ia. The correlations shown here are further strengthened by three test cases, namely SNe 1997cn, 1999da, and 2022xkq, which were not included in the calibration sample.

The work done here shows that 1991bg-like SNe Ia can be standardized and hence used to measure extragalactic distances. However, these width-luminosity relations must first be properly calibrated by compiling a homogeneous sample of 1991bg-like SNe Ia observed by a single survey in a single set of filters. Even then, because 1991bg-like SNe Ia are rarer than normal SNe Ia (15 vs. 70 per cent of all SNe Ia, respectively; Graur et al. 2017b), their inclusion in SN Ia cosmology samples will not make much of a difference. Moreover, their inherent dimness makes them more susceptible to Malmquist bias, which limits their use as probes of dark energy. Finally, as shown here, the quadratic fits used by Burns et al. (2018) to simultaneously fit normal and fast-declining SNe Ia underestimate the absolute magnitudes of SNe Ia in the transition between normal and 1991bg-like SNe Ia, hinting that each of these subtypes should be fit separately.

Instead, I suggest using 1991bg-like SNe Ia as a rung on a new cosmological distance ladder, one that would provide an independent check on the distance ladder based on Cepheids and normal SNe Ia. While extremely successful (e.g., Riess et al. 2022), the latter ladder is biased towards star-forming galaxies, which host young Cepheid variables. 1991bg-like SNe Ia, on the other hand, are mostly found in massive, passive galaxies (Graur et al. 2017b). This makes them less prone to host-galaxy reddening and removes the systematic uncertainty produced by the mass step found in Hubble residuals (e.g., Kelly et al. 2010; Brout & Scolnic 2021; Kelsey et al. 2021, 2023; Meldorf et al. 2023).

Bereft of Cepheids, the galaxies that host 1991bg-like SNe Ia will have to be calibrated by other means, such as surface-brightness fluctuations. Several groups have already attempted to use this method to either measure  $H_0$  directly or to calibrate the host galaxies of normal SNe Ia (e.g., Blakeslee et al. 2021; Jensen et al. 2021; Khetan et al. 2021; Garnavich et al. 2023; Uddin et al. 2023; Wood et al. 2023). A new distance ladder, based on surface-brightness fluctuations (or some other non-Cepheid method) and 1991bg-like SNe Ia could provide an independent measurement of  $H_0$ , a necessary step towards resolving the current 'Hubble tension' (e.g., Di Valentino et al. 2021; Kamionkowski & Riess 2023).

#### **ACKNOWLEDGMENTS**

I thank Chris R. Burns and Saurabh W. Jha for helpful discussions; Willem B. Hoogendam, Jeniveve Pearson, and the CSP for sharing their data with me; and the anonymous referee for their comments. This research has made use of NASA's Astrophysics Data System and the NASA/IPAC Extragalactic Database (NED), which are funded by the National Aeronautics and Space Administration and operated by the California Institute of Technology. For the purpose of open access, the author has applied a Creative Commons Attribution (CC BY) license to any Author Accepted Manuscript version arising.

#### DATA AVAILABILITY

All data used in this work, except for the CSP data shown in Fig. 4, are public and have been published elsewhere. The measurements and fits produced by this work are included in the tables throughout this paper. Any remaining data or measurements will be shared on request to the corresponding author.

#### REFERENCES

```
Ajhar E. A., Tonry J. L., Blakeslee J. P., Riess A. G., Schmidt B. P., 2001,
    ApJ, 559, 584
Avelino A., Friedman A. S., Mandel K. S., Jones D. O., Challis P. J., Kirshner
    R. P., 2019, ApJ, 887, 106
Bernardi M., Alonso M. V., da Costa L. N., Willmer C. N. A., Wegner G.,
    Pellegrini P. S., Rité C., Maia M. A. G., 2002, AJ, 123, 2159
Blakeslee J. P., Lucey J. R., Barris B. J., Hudson M. J., Tonry J. L., 2001,
    MNRAS, 327, 1004
Blakeslee J. P., et al., 2009, ApJ, 694, 556
Blakeslee J. P., et al., 2010, ApJ, 724, 657
Blakeslee J. P., Jensen J. B., Ma C.-P., Milne P. A., Greene J. E., 2021, ApJ,
    911, 65
Blondin S., Tonry J. L., 2007, ApJ, 666, 1024
Brout D., Scolnic D., 2021, ApJ, 909, 26
Brown T. M., et al., 2013, PASP, 125, 1031
Burns C. R., et al., 2011, AJ, 141, 19
Burns C. R., et al., 2014, ApJ, 789, 32
Burns C. R., et al., 2018, ApJ, 869, 56
Cantiello M., Blakeslee J. P., Raimondo G., Mei S., Brocato E., Capaccioli
```

ApJ, 668, 130 Cantiello M., Biscardi I., Brocato E., Raimondo G., 2011, A&A, 532, A154 Cantiello M., et al., 2013, A&A, 552, A106

Cantiello M., Blakeslee J., Raimondo G., Brocato E., Capaccioli M., 2007,

Cardelli J. A., Clayton G. C., Mathis J. S., 1989, ApJ, 345, 245

Chan D. et al. 2022 April 250, 52

Chen P., et al., 2022, ApJS, 259, 53

M., 2005, ApJ, 634, 239

Ciardullo R., Feldmeier J. J., Jacoby G. H., Kuzio de Naray R., Laychak M. B., Durrell P. R., 2002, ApJ, 577, 31

Conley A., et al., 2008, ApJ, 681, 482

Contreras C., et al., 2010, AJ, 139, 519

Courtois H. M., Tully R. B., 2012, ApJ, 749, 174

DES Collaboration et al., 2024, arXiv e-prints, p. arXiv:2401.02929

Di Valentino E., et al., 2021, Classical and Quantum Gravity, 38, 153001

Dwomoh A. M., et al., 2023, arXiv e-prints, p. arXiv:2311.06178

Feldmeier J. J., Jacoby G. H., Phillips M. M., 2007, ApJ, 657, 76

Ferrarese L., et al., 2000, ApJ, 529, 745

Filippenko A. V., et al., 1992a, AJ, 104, 1543

Filippenko A. V., et al., 1992b, ApJ, 384, L15

Filippenko A. V., Li W. D., Treffers R. R., Modjaz M., 2001, in Paczynski B., Chen W.-P., Lemme C., eds, Astronomical Society of the Pacific Conference Series Vol. 246, IAU Colloq. 183: Small Telescope Astronomy on Global Scales. p. 121

```
Foley R. J., et al., 2013, ApJ, 767, 57
```

```
Ganeshalingam M., et al., 2010, ApJS, 190, 418
Garnavich P. M., et al., 2004, ApJ, 613, 1120
Garnavich P., et al., 2023, ApJ, 953, 35
Gómez M., Richtler T., 2004, A&A, 415, 499
Graham A. W., 2002, MNRAS, 334, 859
Graur O., 2022, Supernova. The MIT Press, Cambridge, MA
Graur O., Bianco F. B., Huang S., Modjaz M., Shivvers I., Filippenko A. V.,
    Li W., Eldridge J. J., 2017a, ApJ, 837, 120
Graur O., Bianco F. B., Modjaz M., Shivvers I., Filippenko A. V., Li W.,
    Smith N., 2017b, ApJ, 837, 121
Graur O., et al., 2023, MNRAS, 526, 2977
Guy J., Astier P., Nobili S., Regnault N., Pain R., 2005, A&A, 443, 781
Guy J., et al., 2007, A&A, 466, 11
Hicken M., Wood-Vasey W. M., Blondin S., Challis P., Jha S., Kelly P. L.,
    Rest A., Kirshner R. P., 2009, ApJ, 700, 1097
Höflich P., Gerardy C. L., Fesen R. A., Sakai S., 2002, ApJ, 568, 791
Hoogendam W. B., et al., 2022, ApJ, 928, 103
Jensen J. B., Tonry J. L., Barris B. J., Thompson R. I., Liu M. C., Rieke M. J.,
    Ajhar E. A., Blakeslee J. P., 2003, ApJ, 583, 712
Jensen J. B., et al., 2021, ApJS, 255, 21
Jha S., et al., 2006a, AJ, 131, 527
Jha S., Branch D., Chornock R., Foley R. J., Li W., Swift B. J., Casebeer D.,
    Filippenko A. V., 2006b, AJ, 132, 189
Jha S., Riess A. G., Kirshner R. P., 2007, ApJ, 659, 122
Jordán A., et al., 2005, ApJ, 634, 1002
Jordán A., et al., 2007, ApJS, 171, 101
Kamionkowski M., Riess A. G., 2023, Annual Review of Nuclear and Particle
    Science, 73, 153
Kasliwal M. M., et al., 2008, ApJ, 683, L29
Kelly P. L., Hicken M., Burke D. L., Mandel K. S., Kirshner R. P., 2010, ApJ,
Kelsey L., et al., 2021, MNRAS, 501, 4861
Kelsey L., et al., 2023, MNRAS, 519, 3046
Khetan N., et al., 2021, A&A, 647, A72
Kowalski M., et al., 2008, ApJ, 686, 749
Krisciunas K., et al., 2001, AJ, 122, 1616
Krisciunas K., et al., 2017, AJ, 154, 211
Lagattuta D. J., Mould J. R., Staveley-Smith L., Hong T., Springob C. M.,
    Masters K. L., Koribalski B. S., Jones D. H., 2013, ApJ, 771, 88
Leibundgut B., et al., 1993, AJ, 105, 301
Li W. D., Qiu Y. L., Qiao Q. Y., Zhang Y., Zhou W., Hu J. Y., 1997, IAU Circ.,
    6661, 1
Macri L. M., Stetson P. B., Bothun G. D., Freedman W. L., Garnavich P. M.,
    Jha S., Madore B. F., Richmond M. W., 2001, ApJ, 559, 243
Masters K. L., et al., 2010, ApJ, 715, 1419
Mei S., et al., 2007, ApJ, 655, 144
Meldorf C., et al., 2023, MNRAS, 518, 1985
Mieske S., Hilker M., 2003, A&A, 410, 445
Mieske S., Hilker M., Infante L., 2005, A&A, 438, 103
Misgeld I., Hilker M., 2011, MNRAS, 414, 3699
Modjaz M., Li W., Filippenko A. V., King J. Y., Leonard D. C., Matheson T.,
    Treffers R. R., Riess A. G., 2001, PASP, 113, 308
Nasonova O. G., de Freitas Pacheco J. A., Karachentsev I. D., 2011, A&A,
    532, A104
Neill J. D., Seibert M., Tully R. B., Courtois H., Sorce J. G., Jarrett T. H.,
    Scowcroft V., Masci F. J., 2014, ApJ, 792, 129
Olivares F., Ragosta F., Pignata G., Rodriguez O., Yaron O., 2019, Transient
    Name Server Classification Report, 2019-95, 1
Pan Y. C., Reed D. K., Medallon M. S., Foley R. J., Jha S. W., Rest A., Scolnic
    D., 2017, The Astronomer's Telegram, 10437, 1
Pearson J., et al., 2024, ApJ, 960, 29
Perlmutter S., et al., 1999, ApJ, 517, 565
Phillips M. M., 1993, ApJ, 413, L105
Phillips M. M., Burns C. R., 2017, in Alsabti A. W., Murdin P., eds, , Hand-
    book of Supernovae. p. 2543, doi:10.1007/978-3-319-21846-5_100
Phillips M. M., et al., 1987, PASP, 99, 592
Pskovskii I. P., 1977, Soviet Ast., 21, 675
```

Riess A. G., et al., 1998, AJ, 116, 1009

```
Riess A. G., et al., 2004, ApJ, 607, 665
Riess A. G., et al., 2022, ApJ, 934, L7
Russell D. G., 2002, ApJ, 565, 681
Rust B. W., 1974, PhD thesis, Oak Ridge National Laboratory, Tennessee
Saha A., Thim F., Tammann G. A., Reindl B., Sandage A., 2006, ApJS, 165,
Sakai S., et al., 2000, ApJ, 529, 698
Saulder C., van Kampen E., Chilingarian I. V., Mieske S., Zeilinger W. W.,
    2016, A&A, 596, A14
Schlafly E. F., Finkbeiner D. P., 2011, ApJ, 737, 103
Sorce J. G., Tully R. B., Courtois H. M., 2012, ApJ, 758, L12
Sorce J. G., et al., 2013, ApJ, 765, 94
Sorce J. G., Tully R. B., Courtois H. M., Jarrett T. H., Neill J. D., Shaya E. J.,
    2014, MNRAS, 444, 527
Springob C. M., Masters K. L., Haynes M. P., Giovanelli R., Marinoni C.,
    2009, ApJS, 182, 474
Springob C. M., et al., 2014, MNRAS, 445, 2677
Stritzinger M., et al., 2010, AJ, 140, 2036
Stritzinger M. D., et al., 2011, AJ, 142, 156
Taubenberger S., et al., 2008, MNRAS, 385, 75
Theureau G., Hanski M. O., Coudreau N., Hallet N., Martin J. M., 2007,
    A&A, 465, 71
Tonry J. L., Dressler A., Blakeslee J. P., Ajhar E. A., Fletcher A. B., Luppino
    G. A., Metzger M. R., Moore C. B., 2001, ApJ, 546, 681
Tully R. B., Courtois H. M., 2012, ApJ, 749, 78
Tully R. B., Pierce M. J., 2000, ApJ, 533, 744
Tully R. B., Rizzi L., Shaya E. J., Courtois H. M., Makarov D. I., Jacobs
    B. A., 2009, AJ, 138, 323
Tully R. B., et al., 2013, AJ, 146, 86
Tully R. B., Courtois H. M., Sorce J. G., 2016, AJ, 152, 50
Turatto M., Benetti S., Cappellaro E., Danziger I. J., Della Valle M., Gouiffes
    C., Mazzali P. A., Patat F., 1996, MNRAS, 283, 1
Turatto M., Piemonte A., Benetti S., Cappellaro E., Mazzali P. A., Danziger
    I. J., Patat F., 1998, AJ, 116, 2431
Uddin S. A., et al., 2023, arXiv e-prints, p. arXiv:2308.01875
Valenti S., Sand D., Tartaglia L., Hosseinzadeh G., Arcavi I., Howell D. A.,
    Mccully C., 2017, Transient Name Server Classification Report, 2017-
    613, 1
Villegas D., et al., 2010, ApJ, 717, 603
Vincenzi M., et al., 2024, arXiv e-prints, p. arXiv:2401.02945
Wang X., Wang L., Pain R., Zhou X., Li Z., 2006, ApJ, 645, 488
Wood C., et al., 2023, in American Astronomical Society Meeting Abstracts.
    p. 424.10
Yang J., et al., 2022, ApJ, 938, 83
de Vaucouleurs G., de Vaucouleurs A., Corwin Herold G. J., Buta R. J., Paturel
    G., Fouque P., 1991, Third Reference Catalogue of Bright Galaxies
```

#### APPENDIX A: DISTANCE MODULUS REFERENCES

In this section, I summarize the sources of the various distance moduli measurements used to calculate the weighted means shown in Table 1. The acronyms used in Table A1, below, are: Cepheids (Cep), cosmic microwave background (CMB), dwarf galaxy diameter (DGD), fundamental plane (FP), globular cluster luminosity function (GCLF), globular cluster radius (GCR), planetary nebula luminosity function (PNLF), surface brightness fluctuations (SBF), and the Tully-Fisher relation (TF).

Table A1. Distance modulus references

SN	Host	Method	References
1991bg	NGC 4374	FP GCLF GCR PNLF SBF TF	Blakeslee et al. (2001) Gómez & Richtler (2004); Jordán et al. (2007); Villegas et al. (2010) Jordán et al. (2005) Ferrarese et al. (2000); Ciardullo et al. (2002) Ferrarese et al. (2000); Blakeslee et al. (2001, 2009); Mei et al. (2007); Cantiello et al. (2011) Courtois & Tully (2012)
1998de	NGC 0252	CMB	Modjaz et al. (2001)
1999by	NGC 2841	Cep TF	Macri et al. (2001); Saha et al. (2006) Russell (2002); Tully et al. (2009); Springob et al. (2009); Courtois & Tully (2012); Sorce et al. (2012, 2014)
1999da	NGC 6411	FP SBF	Blakeslee et al. (2001) Blakeslee et al. (2001)
2005bl	NGC 4059	FP TF	Saulder et al. (2016) Theureau et al. (2007)
2006mr	NGC 1316	D-σ DGD FP GCLF GCR PNLF TF	Bernardi et al. (2002) Misgeld & Hilker (2011) Graham (2002) Villegas et al. (2010) Masters et al. (2010) Ciardullo et al. (2002); Feldmeier et al. (2007) Sakai et al. (2000); Tully & Pierce (2000); Theureau et al. (2007); Tully & Courtois (2012) Courtois & Tully (2012); Sorce et al. (2013, 2014); Neill et al. (2014); Tully et al. (2016) Tonry et al. (2001); Ajhar et al. (2001); Jensen et al. (2003); Cantiello et al. (2007) Blakeslee et al. (2009, 2010); Cantiello et al. (2013)
2007ax	NGC 2577	TF	Theureau et al. (2007)
2008R	NGC 1200	FP	Springob et al. (2014)
2015bo	NGC 5490	TF SBF	Theureau et al. (2007) Jensen et al. (2021)
2017ejb	NGC 4696	DGD FP FP+SBF GCLF TF SBF	Misgeld & Hilker (2011) Blakeslee et al. (2001) Tully et al. (2013) Mieske et al. (2005) Theureau et al. (2007); Tully et al. (2016) Tonry et al. (2001); Blakeslee et al. (2001); Mieske & Hilker (2003); Cantiello et al. (2005)
2019so	NGC 4622	FP	Springob et al. (2014)
2021qvv	NGC 4442	GCLF GCR TF SBF	Jordán et al. (2007); Villegas et al. (2010) Jordán et al. (2005) Theureau et al. (2007) Mei et al. (2007); Blakeslee et al. (2009)
2022xkq	NGC 1784	TF	Theureau et al. (2007); Tully et al. (2009); Nasonova et al. (2011); Tully et al. (2013, 2016); Lagattuta et al. (2013) Sorce et al. (2014)

Note. SN 1997cn exploded in the same host galaxy as SN 2015bo, NGC 5490.